Applied Mathematics and Mechanics
(English Edition) Vol. 26 No. 12 Dec. 2005

Published by Shanghai University,
Shanghai, China

©Editorial Committee of Appl. Math. Mech., **ISSN** 0253-4827 **Article ID**: 0253-4827(2005)12-1564-10

DUAL RECIPROCITY BOUNDARY ELEMENT METHOD FOR FLEXURAL WAVES IN THIN PLATE WITH CUTOUT *

GAO Suo-wen (高锁文)[1], WANG Yue-sheng (汪越胜)[1],
ZHANG Zi-mao (章梓茂)[1], MA Xing-rui (马兴瑞)[2]

(1. Institute of Engineering Mechanics, Beijing Jiaotong University, Beijing 100044, P. R. China;
2. China Aerospace Science and Technology Corporation, Beijing 100037, P. R. China)

(Contributed by MA Xing-rui)

Abstract: The theoretical analysis and numerical calculation of scattering of elastic waves and dynamic stress concentrations in the thin plate with the cutout was studied using dual reciprocity boundary element method (DRM). Based on the work equivalent law, the dual reciprocity boundary integral equations for flexural waves in the thin plate were established using static fundamental solution. As illustration, numerical results for the dynamic stress concentration factors in the thin plate with a circular hole are given. The results obtained demonstrate good agreement with other reported results and show high accuracy.

Key words: thin plate; DRM; scattering of flexural wave; dynamic stress concentration

Chinese Library Classification: O347.4 **Document code**: A
2000 Mathematics Subject Classification: 74K20

Introduction

The thin plates are extensively used as components in engineering structures. Arbitrary cavities are inevitably made in the plates in order to satisfy various engineering needs. Hence physical discontinuation is resulted. The dynamic stress concentrations around the cavity in a plate are produced under the load. Therefore capacity of the plate is lowered and its service life is shortened. So in recent mechanics research, many experts have made theoretical analysis, numerical calculation and experimental research in this aspect[1-3].

In the 1960s, Pao[2] first studied the diffraction of flexural wave and dynamic stress concentrations around a circular hole, and proposed the analytic solution and numerical example. In 1982, Liu *et al.* [3] presented a complex function method representing a new

* Received Jun. 25, 2004; Revised Sep. 01, 2005
Project supported by the National Science Fund for Distinguished Young Scholars (No. 10025211) and the Post-Doctoral Science Foundation of China (No. 2003033046)
Corresponding author GAO Suo-wen, Associate Professor, Doctor, E-mail: bjgsw@sina.com

approach to two-dimensional scattering. It was an extension of the complex function method for elastostatics. With the extensive application of elastic wave theory, wave function expansion method, integral transform method, integral equations method and complex function method were developed.

Because of the complexity of the dynamic stress concentrations around a cavity in a plate produced by scattering of elastic waves, satisfactory analytic solution is hard to obtain. Hence, numerical methods are extensively used in this subject. Boundary element method (BEM) is an important numerical method, and it has been developed rapidly in the past 20 years. For the solution to the problems of dynamic or nonhomogeneous equations, many techniques have been developed to overcome the obstacle due to difficulty in finding fundamental solutions and to avoid domain integrals. The DRM proved as a general successful approach[4]. The advantage of DRM is to construct the boundary integral equations by using the simple static fundamental solution of corresponding problems. Thus, domain integral of the inertia term is generated. In order to transform domain integrals into boundary integrals, the reciprocity theorem is used once again, and an expression named radial basis functions (RBF) is also used in the procedure. DRM was first introduced by Nardini & Brebbia[5] to solve dynamic problems in solid mechanics and now it has been extended to a wide range of application.

Kogl *et al.* [6] employed the DRM for the solution of three-dimensional anisotropic free vibration problems. By means of numerical examples, the influence of the internal collocation points on the representation of the mass matrix and the occurrence of complex-valued eigenfrequencies is investigated. Rodriguez *et al.* [7] presented a mesh h-refinement technique based on error bounds for the collocation BEM. In Ref. [8], they extend the refinement technique to the DRM for 2D Poisson problems. Chien *et al.* [9] applied the DRM to the transient analysis of 2D elastodynamic problems. In this work, the second-order ordinary differential equations in the domain formulated by the DRM are solved using the time-discontinuous Galerkin FEM. Itagaki[10] presented a new DRM to solve the modified Helmholtz-type equation, which has a space dependent source term described by a polynomial. This scheme is expanded to solve iteratively the Helmholtz-type eigenvalue problem for a nonuniform media. In Chen's *et al.* [11] paper, true and spurious eigensolutions for a circular cavity using the dual multiple reciprocity method (MRM) are analytically derived and numerically verified by the developed program. Singh *et al.* [12] presented an application of the DRM to inverse heat conduction problems. Albuquerque *et al.* [13,14] discussed the use of DRM for transient problems of anisotropic materials with or without cracks. Chen *et al.* [15] presented a numerical study of convergence properties of the boundary knot method (BKM) applied to the solution of 2D and 3D homogeneous Helmholtz, modified Helmholtz, and convection-diffusion problems. The BKM is a new boundary-type, meshfree radial function basis collocation technique.

Reference[16] studied the theoretical analysis and numerical calculation of scattering of elastic wave and dynamic stress concentrations in the thin plate with a circular hole using BEM. The numerical results are given for the problem. Because dynamic fundamental solution are employed in Ref. [16], the derivation of the formulas and the calculation of the

influence coefficients are very complex and computational efficiency decreases. This paper applies DRM to solve the scattering of flexural wave and dynamic stress concentrations in the thin plate with a circular hole. The problem is simplified and the computing accuracy can be guaranteed.

1 Flexural Wave Equations and Dual Reciprocity Boundary Integral Equations in Thin Plate

The problem of flexural wave in the thin plate can be summed up as solving the middle plane deflection under the conditions of given load and boundary. The governing equation can be expressed as follows:

$$D\nabla^4 W + \rho h \frac{\partial^2 W}{\partial t^2} = q, \tag{1}$$

where ∇^4 is the biharmonic operator, ρ is the plate mass density, D is its flexural rigidity, h is its thickness, q is the transverse load, W is the deflection of plate.

In Eq.(1), taking $q = 0$, assuming this problem to be a simple harmonic motion (SHM) with the frequency of ω in time-field, that is to find the stable solution. Then the displacement components determined by steady-state flexural waves can be expressed as

$$u_x = -z\frac{\partial W}{\partial x}, \quad u_y = -z\frac{\partial W}{\partial y}, \quad u_z = W = w(x,y)e^{-i\omega t}, \tag{2}$$

where ω is the circular frequency of flexural waves, and $w(x,y)$ should satisfy the following equation:

$$\nabla^4 w - \lambda^4 w = 0 \tag{3}$$

with $\lambda^4 = \frac{\rho h}{D}\omega^2$, and λ is the wave number.

Rewrite Eq.(3) as

$$\nabla^4 w = \lambda^4 w. \tag{4}$$

Taking the fundamental solution of Eq.(4) w^* as the solution of

$$\nabla^4 w^* = \delta(r - r_1). \tag{5}$$

The solution of Eq.(5) can be expressed as

$$w^*(Q,P) = \frac{r^2}{8\pi}\ln r, \tag{6}$$

where $r = |PQ| = \sqrt{(x_Q - x_P)^2 + (y_Q - y_P)^2}$ is the distance from singular source point P to field point Q, P and Q are arbitrary interior source point and field point, respectively, p and q are arbitrary source point and field point on the boundary, respectively.

In order to avoid domain integrals in the formulation of the boundary integral equation, the following approximation for w at the right side of Eq.(4) is then proposed:

$$\tilde{w} = \sum_{j=1}^{M} \alpha_j f_j, \tag{7}$$

where f_j is the function of the distance between the point Q and P, and $\alpha_j (j = 1,2,\cdots,M)$ is a set of unknown coefficients, M is the total number of nodes in the problem. If there are N boundary nodes and L internal nodes, M is equal to $N + L$. If we can find a function $\hat{w}_j$ associated with each f_j satisfying the relation

$$\nabla^4 \hat{w}_j = f_j. \tag{8}$$

Equation (7) can be expressed as

$$\tilde{w} = \sum_{j=1}^{M} \alpha_j (\nabla^4 \hat{w}_j). \tag{9}$$

Using Eq.(9) to replace of deflection w on the right side of Eq.(4) to give the following expression:

$$\nabla^4 w = \lambda^4 \sum_{j=1}^{M} \alpha_j (\nabla^4 \hat{w}_j). \tag{10}$$

Equation (10) can be multiplied by the fundamental solution w^* and integrated over the domain, producing

$$\int_\Omega w^* \nabla^4 w \mathrm{d}\Omega = \sum_{j=1}^{M} \lambda^4 \alpha_j \int_\Omega w^* \nabla^4 \hat{w}_j \mathrm{d}\Omega. \tag{11}$$

Using the Betti-Rayleigh reciprocal theorem into both sides of Eq.(11) and noticing Eq.(5) and character of δ function, produces the following integral equation:

$$\begin{aligned} C(P)w(P) &+ \int_\Gamma V_n^* w \mathrm{d}\Gamma - \int_\Gamma M_n^* \frac{\partial w}{\partial n_q} \mathrm{d}\Gamma + \int_\Gamma \frac{\partial w^*}{\partial n_q} M_n \mathrm{d}\Gamma - \int_\Gamma w^* V_n \mathrm{d}\Gamma \\ &= \sum_{j=1}^{M} \lambda^4 \alpha_j \Big[C(P)\hat{w}_j(P) + \int_\Gamma V_n^* \hat{w}_j \mathrm{d}\Gamma - \int_\Gamma M_n^* \frac{\partial \hat{w}_j}{\partial n_q} \mathrm{d}\Gamma \\ &\quad + \int_\Gamma \frac{\partial w^*}{\partial n_q} \hat{M}_{nj} \mathrm{d}\Gamma - \int_\Gamma w^* \hat{V}_{nj} \mathrm{d}\Gamma \Big]. \end{aligned} \tag{12}$$

Equation (12) is the boundary integral equation to resolve the deflection of any point P in the thin plate field. The constant $C(P)$ depends on the location of point P, $C(P) = 1$ for points in the domain, and for points on the boundary it is the included angle between the two elements that join at the node point P. Thus, $C(P) = \theta/2\pi$. $V_n^* = V_n[w^*(p,q)]$, $M_n^* = M_n[w^*(p,q)]$, $M_n = M_n[w(q)]$, $V_n = V_n[w(q)]$, $\hat{M}_{nj} = M_n[\hat{w}_j(q)]$, $\hat{V}_{nj} = V_n[\hat{w}_j(q)]$. M_n and V_n are boundary condition operators. Its explicit expression can be found in Ref. [16]. Note that Eq.(12) only involves boundary integrals but not domain integrals. Therefore, discretization of the domain interior is avoided, which keeps the attraction of boundary element, *i. e.*, its discretization only at the boundary, and computational efficiency increases. Furthermore, the accuracy of the method is examined through numerical example.

For any point p on the smooth boundary, Eq.(12) becomes

$$\begin{aligned} \frac{1}{2} w(p) &+ \int_\Gamma V_n^* w \mathrm{d}\Gamma - \int_\Gamma M_n^* \frac{\partial w}{\partial n_q} \mathrm{d}\Gamma + \int_\Gamma \frac{\partial w^*}{\partial n_q} M_n \mathrm{d}\Gamma - \int_\Gamma w^* V_n \mathrm{d}\Gamma \\ &= \sum_{j=1}^{M} \lambda^4 \alpha_j \Big[\frac{1}{2} \hat{w}_j(p) + \int_\Gamma V_n^* \hat{w}_j \mathrm{d}\Gamma - \int_\Gamma M_n^* \frac{\partial \hat{w}_j}{\partial n_q} \mathrm{d}\Gamma + \int_\Gamma \frac{\partial w^*}{\partial n_q} \hat{M}_{nj} \mathrm{d}\Gamma - \int_\Gamma w^* \hat{V}_{nj} \mathrm{d}\Gamma \Big]. \end{aligned} \tag{13}$$

By differentiating Eq.(13) with respect to the outward normal n_p at the point p on the boundary, one can get another boundary integral equation, which is linearly independent with Eq.(13):

$$\frac{1}{2} \frac{\partial w(p)}{\partial n_p} + \int_\Gamma \frac{\partial V_n^*}{\partial n_p} w \mathrm{d}\Gamma - \int_\Gamma \frac{\partial M_n^*}{\partial n_p} \frac{\partial w}{\partial n_q} \mathrm{d}\Gamma + \int_\Gamma \frac{\partial^2 w^*}{\partial n_q \partial n_p} M_n \mathrm{d}\Gamma - \int_\Gamma \frac{\partial w^*}{\partial n_p} V_n \mathrm{d}\Gamma$$

$$= \sum_{j=1}^{M} \lambda^4 \alpha_j \left[\frac{1}{2} \frac{\partial \hat{w}_j(p)}{\partial n_p} + \int_\Gamma \frac{\partial V_n^*}{\partial n_p} \hat{w}_j \mathrm{d}\Gamma - \int_\Gamma \frac{\partial M_n^*}{\partial n_p} \frac{\partial \hat{w}_j}{\partial n_q} \mathrm{d}\Gamma \right.$$
$$\left. + \int_\Gamma \frac{\partial^2 w^*}{\partial n_q \partial n_p} \hat{M}_{nj} \mathrm{d}\Gamma - \int_\Gamma \frac{\partial w^*}{\partial n_p} \hat{V}_{nj} \mathrm{d}\Gamma \right]. \tag{14}$$

Equations (13) and (14) constitute a system of simultaneous integral equations in terms of the four basic boundary values, *i. e.*, deflection w, normal slope $\partial w/\partial n$, normal bending moment M_n and equivalent shear force V_n. For each boundary point, two variables are known and another two variables are unknown generally. The plate boundary is divided into N elements, and interpolating function is chosen in each element, then the problem is translated into solving the $2N$-th order system of linear algebraic equations. However, the unknown coefficients α_j and function $\hat{w}_j$ are included in this system of equations. So choosing suitable f_j is necessary. Numerical calculation illustrates that f_j can be chosen as

$$f_j = 1 - r - r^2, \tag{15}$$

where r is the distance between two points. In this case, a function $\hat{w}_j$ defined by Eq.(8) has the following form:

$$\hat{w}_j = \frac{1}{64} r^4 - \frac{1}{225} r^5 - \frac{1}{576} r^6. \tag{16}$$

The unknown coefficients α_j defined by Eq.(7) are determined through the following procedure. Using Eq.(7) into M points, which combines N boundary nodes and L interior nodes, and replacing $\tilde{w}$ by the deflection of M points. Eq.(7) is represented in matrix form as follows:

$$\boldsymbol{w} = \boldsymbol{F}\boldsymbol{\alpha}. \tag{17}$$

If the matrix $\boldsymbol{F}$ has its inverse $\boldsymbol{F}^{-1}$, a set of the unknown coefficients $\boldsymbol{\alpha}$ is obtained by

$$\boldsymbol{\alpha} = \boldsymbol{F}^{-1}\boldsymbol{w}. \tag{18}$$

Equation (18) indicates that $\boldsymbol{\alpha}$ can be expressed as the deflection of M points. So $4N + L$ unknown variables are involved in the system of Eqs.(13) and (14). After introducing $2N$ boundary conditions, $2N + L$ unknown variables still remain. It means that it needs $2N + L$ equations to obtain the solution of problem. We solve simultaneously Eqs.(13) and (14) and calculating equations for L interior points can be given from Eq.(12).

2 Discretization for Boundary Integral Equations

In Eqs.(13) and (14) notations a_i are introduced, and their explicit expression can be found from Ref. [16]. Similar notations b_i are introduced into Eq.(12). We define $\theta = \partial w/\partial n_q = \partial w/\partial n_p, \hat{\theta}_j = \partial \hat{w}_j/\partial n_q = \partial \hat{w}_j/\partial n_p$.

When Eqs.(12), (13) and (14) are solved using the dual reciprocity boundary element method, the boundary of the plate is discretized into finite boundary elements and finite interior points are chosen. The w, $\partial w/\partial n$, V_n and M_n are considered as mutually independent variables, and their differential relations are not considered. Using the numerical value of variables at the points as unknown, the boundary integral equations (12), (13) and (14) are discretized into the system of linear algebraic equations by means of the interpolating functions.

Equations (12), (13) and (14) can be discretized, respectively, as

$$c_i w_i - \sum_{q=1}^{N}\int_{\Gamma_q} V_{n_q} b_1 \mathrm{d}s + \sum_{q=1}^{N}\int_{\Gamma_q} M_{n_q} b_2 \mathrm{d}s - \sum_{q=1}^{N}\int_{\Gamma_q} \theta_q b_3 \mathrm{d}s + \sum_{q=1}^{N}\int_{\Gamma_q} w_q b_4 \mathrm{d}s$$
$$= \sum_{j=1}^{M} \lambda^4 \alpha_j \Big[c_i \hat{w}_{ij} - \sum_{q=1}^{N}\int_{\Gamma_q} \hat{V}_{n_q j} b_1 \mathrm{d}s + \sum_{q=1}^{N}\int_{\Gamma_q} \hat{M}_{n_q j} b_2 \mathrm{d}s$$
$$- \sum_{q=1}^{N}\int_{\Gamma_q} \hat{\theta}_{qj} b_3 \mathrm{d}s + \sum_{q=1}^{N}\int_{\Gamma_q} \hat{w}_{qj} b_4 \mathrm{d}s \Big], \tag{19}$$

$$\frac{1}{2} w_p - \sum_{q=1}^{N}\int_{\Gamma_q} V_{n_q} a_1 \mathrm{d}s + \sum_{q=1}^{N}\int_{\Gamma_q} M_{n_q} a_2 \mathrm{d}s - \sum_{q=1}^{N}\int_{\Gamma_q} \theta_q a_3 \mathrm{d}s + \sum_{q=1}^{N}\int_{\Gamma_q} w_q a_4 \mathrm{d}s$$
$$= \sum_{j=1}^{M} \lambda^4 \alpha_j \Big[\frac{1}{2} \hat{w}_{pj} - \sum_{q=1}^{N}\int_{\Gamma_q} \hat{V}_{n_q j} a_1 \mathrm{d}s + \sum_{q=1}^{N}\int_{\Gamma_q} \hat{M}_{n_q j} a_2 \mathrm{d}s$$
$$- \sum_{q=1}^{N}\int_{\Gamma_q} \hat{\theta}_{qj} a_3 \mathrm{d}s + \sum_{q=1}^{N}\int_{\Gamma_q} \hat{w}_{qj} a_4 \mathrm{d}s \Big], \tag{20}$$

$$\frac{1}{2} \theta_p - \sum_{q=1}^{N}\int_{\Gamma_q} V_{n_q} a_5 \mathrm{d}s + \sum_{q=1}^{N}\int_{\Gamma_q} M_{n_q} a_6 \mathrm{d}s - \sum_{q=1}^{N}\int_{\Gamma_q} \theta_q a_7 \mathrm{d}s + \sum_{q=1}^{N}\int_{\Gamma_q} w_q a_8 \mathrm{d}s$$
$$= \sum_{j=1}^{M} \lambda^4 \alpha_j \Big[\frac{1}{2} \hat{\theta}_{pj} - \sum_{q=1}^{N}\int_{\Gamma_q} \hat{V}_{n_q j} a_5 \mathrm{d}s + \sum_{q=1}^{N}\int_{\Gamma_q} \hat{M}_{n_q j} a_6 \mathrm{d}s$$
$$- \sum_{q=1}^{N}\int_{\Gamma_q} \hat{\theta}_{qj} a_7 \mathrm{d}s + \sum_{q=1}^{N}\int_{\Gamma_q} \hat{w}_{qj} a_8 \mathrm{d}s \Big], \tag{21}$$

where Γ_q is the length of the q-th element, $\int_{\Gamma_q}(\cdot)\mathrm{d}s$ denotes the integration for the q-th element, and in Eqs.(20) and (21), $p = 1,2,\cdots,N$.

In the case of the constant elements, the values of variables are assumed to be constant over each element and equal to the value at the mid-element node. Note that for this type of element (*i. e.*, constant element) the boundary is always smooth at the nodes as these are located at the center of the elements, hence the constant $C(p)$ is always 1/2. If each of the vectors $\hat{\boldsymbol{w}}_j, \hat{\boldsymbol{\theta}}_j, \hat{\boldsymbol{M}}_{nj}$ and $\hat{\boldsymbol{V}}_{nj}$ is considered to be one column of the matrices $\hat{\boldsymbol{w}}, \hat{\boldsymbol{\theta}}, \hat{\boldsymbol{M}}_n$ and $\hat{\boldsymbol{V}}_n$, respectively, then Eqs.(19), (20) and (21) may be written in matrix form:

$$\boldsymbol{I}\boldsymbol{w} + \boldsymbol{B}_4\boldsymbol{w} - \boldsymbol{B}_3\boldsymbol{\theta} + \boldsymbol{B}_2\boldsymbol{M}_n - \boldsymbol{B}_1\boldsymbol{V}_n = (\boldsymbol{I}\hat{\boldsymbol{w}} + \boldsymbol{B}_4\hat{\boldsymbol{w}} - \boldsymbol{B}_3\hat{\boldsymbol{\theta}} + \boldsymbol{B}_2\hat{\boldsymbol{M}}_n - \boldsymbol{B}_1\hat{\boldsymbol{V}}_n)\lambda^4\boldsymbol{\alpha}, \tag{22}$$

$$\boldsymbol{A}_4\boldsymbol{w} - \boldsymbol{A}_3\boldsymbol{\theta} + \boldsymbol{A}_2\boldsymbol{M}_n - \boldsymbol{A}_1\boldsymbol{V}_n = (\boldsymbol{A}_4\hat{\boldsymbol{w}} - \boldsymbol{A}_3\hat{\boldsymbol{\theta}} + \boldsymbol{A}_2\hat{\boldsymbol{M}}_n - \boldsymbol{A}_1\hat{\boldsymbol{V}}_n)\lambda^4\boldsymbol{\alpha}, \tag{23}$$

$$\boldsymbol{A}_8\boldsymbol{w} - \boldsymbol{A}_7\boldsymbol{\theta} + \boldsymbol{A}_6\boldsymbol{M}_n - \boldsymbol{A}_5\boldsymbol{V}_n = (\boldsymbol{A}_8\hat{\boldsymbol{w}} - \boldsymbol{A}_7\hat{\boldsymbol{\theta}} + \boldsymbol{A}_6\hat{\boldsymbol{M}}_n - \boldsymbol{A}_5\hat{\boldsymbol{V}}_n)\lambda^4\boldsymbol{\alpha}. \tag{24}$$

In the above equations, the terms $C(p)$ have been incorporated onto the principal diagonal of corresponding matrix.

In Eq.(22), the matrix $\boldsymbol{I}$ is an $L \times L$ unit matrix, the vector $\boldsymbol{w}$ multiplied by $\boldsymbol{I}$ is the deflection at L interior points, L interior points and N boundary point generate $L \times N$ influence coefficient matrices $\boldsymbol{B}_i (i = 1,2,3,4)$ by the fundamental solution, the vectors $\boldsymbol{w}, \boldsymbol{\theta}, \boldsymbol{M}_n$ and $\boldsymbol{V}_n$ multiplied, respectively, by $\boldsymbol{B}_i$ are the unknown variables at N boundary points, L interior points and M all points produce $L \times M$ known matrix $\hat{\boldsymbol{w}}$ multiplied by $\boldsymbol{I}$ from Eq.(16), and the N boundary points and the M all points create $N \times M$ known matrices $\hat{\boldsymbol{w}}, \hat{\boldsymbol{\theta}}, \hat{\boldsymbol{M}}_n$ and $\hat{\boldsymbol{V}}_n$ multiplied, respectively, by $\boldsymbol{B}_i$ from Eq.(16). α are M (total of the points) unknown coefficients, it can be expressed by the deflections at M points from Eq.(18). In Eqs.(23)

and (24), $A_i(i = 1,2,\cdots,8)$ are $N \times N$ coefficient matrices (see Ref. [16]), and others have the same meaning as ones in Eq.(22).

The following matrix notation are defined:

$$S_1 = A_4\hat{w} - A_3\hat{\theta} + A_2\hat{M}_n - A_1\hat{V}_n, \quad S_2 = A_8\hat{w} - A_7\hat{\theta} + A_6\hat{M}_n - A_5\hat{V}_n,$$

$$S_3 = I\hat{w} + B_4\hat{w} - B_3\hat{\theta} + B_2\hat{M}_n - B_1\hat{V}_n,$$

$$A_{48} = \begin{bmatrix} A_4 \\ A_8 \end{bmatrix}, \quad A_{37} = \begin{bmatrix} A_3 \\ A_7 \end{bmatrix}, \quad A_{26} = \begin{bmatrix} A_2 \\ A_6 \end{bmatrix}, \quad A_{15} = \begin{bmatrix} A_1 \\ A_5 \end{bmatrix}, \quad S_{12} = \begin{bmatrix} S_1 \\ S_2 \end{bmatrix},$$

and noticing Eq.(18), Eqs.(22), (23) and (24) can be written in the following matrix form:

$$\begin{bmatrix} A_{48} & 0 \\ B_4 & I \end{bmatrix}\begin{Bmatrix} w^b \\ w^i \end{Bmatrix} - \begin{bmatrix} A_{37} & 0 \\ B_3 & 0 \end{bmatrix}\begin{Bmatrix} \theta^b \\ 0 \end{Bmatrix} + \begin{bmatrix} A_{26} & 0 \\ B_2 & 0 \end{bmatrix}\begin{Bmatrix} M_n^b \\ 0 \end{Bmatrix} - \begin{bmatrix} A_{15} & 0 \\ B_1 & 0 \end{bmatrix}\begin{Bmatrix} V_n^b \\ 0 \end{Bmatrix}$$

$$= \lambda^4 \begin{bmatrix} S_{12} \\ S_3 \end{bmatrix} F^{-1} \begin{Bmatrix} w^b \\ w^i \end{Bmatrix}, \tag{25}$$

where the superscript b denotes value at the boundary node and the superscript i denotes value at the interior node.

After the deflection, normal slope, normal bending moment and equivalent shear force at each boundary node and the deflection of the L interior nodes are obtained from Eq.(25), the deflection of any interior point can be solved by Eq.(19).

In order to solve bending moments of the interior points, one can make use of the deflections of the interior points to do calculus of differences based on the differential relationship between the bending moment and the deflection. The value of the bending moment at any interior point can be obtained easily in this way. After the normal and tangential bending moments near the boundary are solved, the dynamic stress (bending moment) concentration factors around the hole can be obtained.

3 Dynamic Stress Concentration Factors of Thin Plate With Circular Hole

Considering an infinite thin plate with a circular hole inside, the boundaries of the hole are free. The total of the moments and the shears is zero, respectively. Now suppose there is a flexural wave of steady state which comes in from limitless distance from the plate, and the incident direction is consistent with x-axis. The incident wave can be written as

$$w^{(i)} = w_0 e^{i\lambda x}. \tag{26}$$

Taking the amplitude of incident wave $w_0 = 1$, under the polar coordinate system, Eq.(26) becomes $w^{(i)} = e^{i\lambda r\cos\theta}$. Using boundary condition operator under polar coordinate system, the boundary moment and shear caused by the incident wave are expressed as

$$M_n = \frac{D(1-\mu)\lambda^2}{2} e^{i\lambda r\cos\theta}\left(\cos 2\theta + \frac{1+\mu}{1-\mu}\right), \tag{27}$$

$$V_n = -Di\lambda^3\cos\theta e^{i\lambda r\cos\theta} + \frac{D\lambda^2(1-\mu)}{2r}(2\cos 2\theta - i\lambda r\sin\theta\sin 2\theta)e^{i\lambda r\cos\theta}. \tag{28}$$

After Eqs.(27) and (28) are discretized in the same way and substituted into Eq.(25),

one can get the boundary variables around the hole and the deflections of the chosen interior points.

From the definition of the dynamic stress concentration factor, it is known that the dynamic moment concentration factors are the ratios of the amplitude of the moment produced by the full-waves at some point to that produced by the incident waves at the same point around the hole

$$M_\theta^* = M_\theta / M_0. \tag{29}$$

The amplitude of moment produced by incident waves is

$$M_0 = D\lambda^2 w_0 = D\lambda^2. \tag{30}$$

The M_θ is determined by the node value from Eq.(25).

Dynamic moment concentration factors can be solved from Eq.(29).

4 Numerical Examples

Take the radius of the circular hole $R = 1$, Poisson's ratio $\mu = 0.3$, $f = 1 - r - r^2$. Divide the boundary of the circular hole into 60 constant elements, and take 60 interior points, as shown in Fig. 1. When different values are given to nondimensional wave number λ, the change of the dynamic moment concentration factors M_θ^* around the hole are shown in Fig. 2 – Fig. 6, respectively. The values of M_θ^* are symmetrical to x-axis. The numerical results of the dynamic moment concentration factors are given in Table 1 by choosing two kinds of f-function and the different wave number λ.

Table 1 Dynamic moment factors ($\theta = \pi/2$)

λ	$f = 1 + r$	$f = 1 - r - r^2$	Ref. [16]
0.1	1.828 5	1.830 1	1.836 0
0.5	1.668 1	1.669 2	1.671 0
1.0	1.645 2	1.643 7	1.642 0
2.0	1.643 9	1.645 8	1.655 0
3.0	1.647 5	1.648 3	1.650 0
5.0	1.650 3	1.650 9	1.652 0

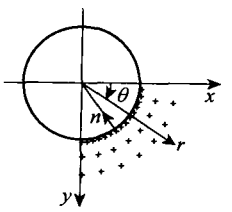

Fig. 1 Element division

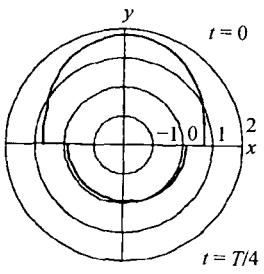

Fig. 2 $\lambda = 0.1$ Dynamic moment factors

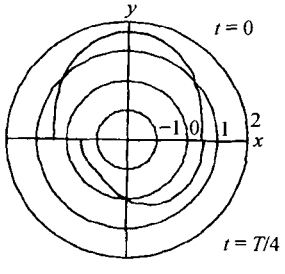

Fig. 3 $\lambda = 0.5$ Dynamic moment factors

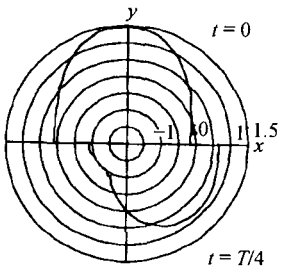

Fig. 4 $\lambda = 1.0$ Dynamic moment factors

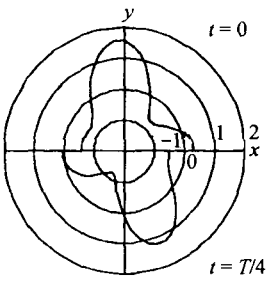

Fig. 5 λ = 3.0 Dynamic moment factors

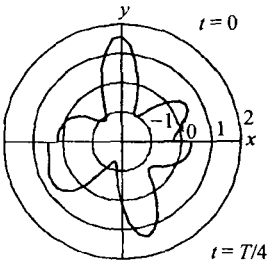

Fig. 6 λ = 5.0 Dynamic moment factors

5 Conclusions

Numerical results show that the dynamic stress concentration factors of the plate with circular hole decrease as increasing the nondimensional wave number. The dynamic stress concentration factor is bigger when the wave frequency is lower, about 1.85; the dynamic stress concentration factors change around 1.65 when the wave frequency is higher ($\lambda > 2$).

This paper is based on the DRM, the boundary integral equations of the flexural waves in the thin plate are established. In order to compare conveniently, the constant element scheme is employed for the discretization of the boundary integral equations, and the system of linear algebraic equations are obtained. The deflections at the interior points are included in the system of linear algebraic equations. So the boundary deflections, boundary forces and interior points deflections can be solved simultaneously. In order to testify the accuracy and the availability of the present method, the same numerical examples as Ref. [16] are given. The numerical results are as accurate as in Ref. [16], and the theoretical derivation and numerical calculation of the DRM are simpler than the direct dynamic boundary element method of ones.

Acknowledgements The authors are pleased to acknowledge the BJTU paper Foundation of China (PD176 - 177) for supporting this research work.

References:

[1] Wang Duo, Ma Xingrui, Liu Diankui. *The Newest Advance of Elastodynamics*[M]. Science Press, Beijing, 1995, 1 - 106 (in Chinese).

[2] Pao Y H. Dynamical stress concentration in an elastic plate[J]. *J Appl Mech*, 1962, **29**(2): 299 - 305.

[3] Liu Diankui, Gai Bingzheng, Tao Guiguan. Application of the method of complex functions to dynamic stress concentrations[J]. *Wave Motion*, 1982, **4**(3): 293 - 304.

[4] Partridge P W, Brebbia C A, Wrobel L C. *Dual Reciprocity Boundary Element Method*[M]. Southampton Boston: Comput Mech Pub, 1992, 1 - 176.

[5] Nardini D, Brebbia C A. A new approach to free vibration analysis using boundary elements [A]. In: Brebbia C A (ed). *Boundary Elements Methods in Engineering*[C]. Springer-Verlag, Berlin, 1982, 312 - 326.

[6] Kogl M, Gaul L. Free vibration analysis of anisotropic solids with the boundary element

method[J]. *Engineering Analysis with Boundary Elements*,2003,**27**(2):107 - 114.

[7] Rodriguez J J,Power H. *H*-adaptive mesh refinement strategy for the boundary element method based on local error analysis[J]. *Engineering Analysis with Boundary Elements*,2001,**25**(7):565 - 579.

[8] Rodriguez J J,Power H. An adaptive dual reciprocity scheme for the numerical solution of the Poisson equation[J]. *Engineering Analysis with Boundary Elements*,2002,**26**(4):283 - 300.

[9] Chien C C,Chen Y H,Chuang C C. Dual reciprocity BEM analysis of 2D transient elastodynamic problems by time-discontinuous Galerkin FEM[J]. *Engineering Analysis with Boundary Elements*,2003,**27**(6):611 - 624.

[10] Itagaki M. Advanced dual reciprocity method based on polynomial source and its application to eigenvalue problem for nonuniform media[J]. *Engineering Analysis with Boundary Elements*,2000,**24**(2):169 - 176.

[11] Chen J T,Kuo S R,Chung I L,*et al*. Study on the true and spurious eigensolutions of two-dimensional cavities using the dual multiple reciprocity method[J]. *Engineering Analysis with Boundary Elements*,2003,**27**(7):655 - 670.

[12] Singh K M,Tanaka M. Dual reciprocity boundary element analysis of inverse heat conduction problems[J]. *Comput Methods Appl Mech Engrg*,2001,**190**(40/41):5283 - 5295.

[13] Albuquerque E L, Sollero P, Aliabadi M H. The boundary element method applied to time dependent problems in anisotropic materials[J]. *Internat J Solids and Structres*,2002,**39**(5):1405 - 1422.

[14] Albuquerque E L, Sollero P, Fedelinski P. Dual reciprocity boundary element method in Laplace domain applied to anisotropic dynamic crack problems[J]. *Computers and Structures*,2003,**81**(17):1703 - 1713.

[15] Chen W,Hon Y C. Numerical investigation on convergence of boundary knot method in the analysis of homogeneous Helmholtz, modified Helmholtz, and convection-diffusion problems [J]. *Comput Methods Appl Mech Engrg*,2003,**192**(15):1859 - 1875.

[16] Gao Suowen,Wang Benli,Ma Xingrui. Scattering of elastic wave and dynamic stress concentrations in the thin plate with a circular hole[J]. *Engineering Mechanics*,2001,**23**(2):14 - 20 (in Chinese).